Han *et al. Chin. J. Mech. Eng.* (2019) 32:99
https://doi.org/10.1186/s10033-019-0411-1

Chinese Journal of Mechanical Engineering

ORIGINAL ARTICLE Open Access

On the Loads for Strength Design of Cutterhead of Full Face Rock Tunnel Boring Machine

Meidong Han[1,2], Zongxi Cai[2*] and Chuanyong Qu[2]

Abstract

Cutterhead loads are the key mechanical parameters for the strength design of the full face hard rock tunnel boring machine (TBM). Due to the brittle rock-breaking mechanism, the excavation loads acting on cutters fluctuate strongly and show some randomness. The conventional method that using combinations of some special static loads to perform the strength design of TBM cutterhead may lead to strength failure during working practice. In this paper, a three-dimensional finite element model for coupled Cutterhead–Rock is developed to determine the cutterhead loads. Then the distribution characteristics and the influence factors of cutterhead loads are analyzed based on the numerical results. It is found that, as time changes, the normal and tangential forces acting on cutters and the total torque acting on the cutterhead approximately distribute log normally, while the total thrusts acting on the cutterhead approximately show a normal distribution. Furthermore, the statistical average values of cutterhead loads are proportional to the uniaxial compressive strength (UCS) of cutting rocks. The values also change with the penetration and the diameter of cutterhead following a power function. Based on these findings, we propose a three-parameter model for the mean of cutterhead loads and a method of generating the random cutter forces. Then the strength properties of a typical cutterhead are analyzed in detail using loads generated by the new method. The optimized cutterhead has been successfully applied in engineering. The method in this paper may provide a useful reference for the strength design of TBM cutterhead.

Keywords: TBM cutterhead, Strength design, Numerical simulation, Three-parameter model, Random cutter forces

1 Introduction

TBM is widely used in the construction of various types of hard rock tunnels. The working performance of cutterhead, which is the key tunneling component of TBM, directly affects the efficiency and safety of construction [1, 2]. Due to the complex geology, such as crumbly strata, super hard rock and jointed rock, cutterhead bears large thrust, strong torque and impact cutter loads. Additionally the brittle rock-breaking mechanism and the inappropriate operating parameters may also result in severe vibration of cutterheads of TBM, which would lead to serious strength failure. Therefore, analyzing the strength property with a certain static load, which is commonly used in the current TBM design, may be unable to fulfill the strength requirement of cutterhead accurately in working condition. Thus, how to impose those loads is essential for the strength design of TBM cutterhead.

However, restricted by the closed and complex underground environment, it is difficult to observe the cutterhead loads directly in tunneling process. Thus, in the early years, researches on cutterhead loads are mainly performed experimentally and theoretically focusing on the cutting forces of the single cutter. Roxborough et al. [3] analyzed cutting forces on a wedge-shaped cutter taking into account the contact area and the UCS of rock. Rostami [4] put forward Colorado School of Mines (CSM) force prediction model based on linear cutting machine (LCM). It's one of the most commonly used formulas in estimating cutter wear and optimizing

*Correspondence: zxcai@tju.edu.cn
[2] School of Mechanical Engineering, Tianjin University, Tianjin 300350, China
Full list of author information is available at the end of the article

cutter layout [5–7]. Using the broken theory of interaction of compression and shearing, Xia et al. [8], established a three-axis force rotary cutting mechanical model of disc cutter. Based on dense core theory, Huo et al. [9] proposed a multi-stage rock fragmentation load prediction model. In addition, with a full-scale rotary cutting machine (RCM), Geng et al. [10] investigated the cutting forces of TBM gage cutters and found that the cutting forces of the gage cutter were lower than those of the normal cutter. Upon this finding, a design scheme of multi-stage cutterhead was proposed [11]. Recently, with the increasing computational capability and the development of sophisticated material models, numerical methods are widely used to better analyze cutting forces. Xia et al. [12], established a finite element model for the rock fragmentation of the center cutter, and studied the formation mechanism and change law of the side force on the center cutter. Tan et al. [13], simulated the construction process of concrete rolling by a disc cutter and pointed out that the three-axis force on the cutter obviously presented the characteristic of a step change. Furthermore, the rock-breaking process by multi cutters was simulated, and the effect of cutter spacing on the cutting forces were discussed [14, 15].

Taking advantage of the cutting forces on the single cutter, some researchers calculated the total loads acting on the cutterhead. Based on the CSM model mentioned above, Liu et al. [6], calculated the cutterhead loads by linear superposition of cutter forces. Using the same method, Zhou et al. [16], proposed a new model to predict the total thrust acting on TBM. However, due to the neglecting of the great differences of cutting forces on different cutters, these models could only provide a relatively rough estimation of the average loads. In addition to these simplified calculation model, the available engineering data were employed for studying the cutterhead loads. Farmer et al. [17], analyzed the variation of cutterhead loads with the rock strength, Nelson et al. [18] analyzed a large number of TBM project data and found that the advancing distance per revolution had a significant effect on thrust. Upon the statistical results of 262 TBMs manufactured after 1985, Ates et al. [19] concluded that cutterhead torque was highly correlated with the TBM diameter, and also related with rock strength and geological discontinuities. Analysis of these studies indicates that cutterhead loads are very complicated mechanical quantities, they depend largely on the geological conditions, operating parameters and structural features.

Comparing to the cutter forces which have been well studied using experimental, numerical and theoretical methods, the cutterhead loads are relatively less-investigated, with only a few qualitative results presented. However, the cutterhead loads are more important to TBM design. They are more than the summary of the cutter forces. Currently, there is still no quantitative model for cutterhead loads of TBM that comprehensively reflects the effects of geological conditions, equipment structures, and operational status on the loads. In addition, the distribution characteristics of the cutterhead loads are not clear yet. To obtain the cutterhead loads for effective strength design, in this paper, a three-dimensional finite element model for coupled Cutterhead–Rock is established firstly. Then the distribution characteristics and the influencing factors of the cutterhead loads are investigated based on the simulation results. And a three-parameter model for the mean of cutterhead loads and the method of generating the random cutter forces are proposed. Finally, a new method is developed to analyze the strength for TBM cutterhead.

2 Simulation of Cutterhead Loads in TBM Tunneling

2.1 Material Model of Rock

Generally speaking, cutterhead loads depend on the counterforce of rock in tunneling process. So, in order to obtain the cutterhead loads, the tunneling process should be simulated firstly. To describe the mechanical behavior of rock in the tunneling process, the rock material model needs contain three parts, namely, a constitutive equation describing the stress-strain relationship, a damage law describing the degradation of rock stiffness, and separation criteria describing the separation of rock fragments.

The modified Mohr-Coulomb model [20] which combines the conventional Mohr-Coulomb criterion with the maximal tensile stress criterion, is employed to account for the nonlinear behavior of rock in a tunneling process. This model overcomes two major shortcomings of the Mohr-Coulomb model that exist in finite element analysis packages, namely it describes the tensile strength of material at a higher level and there are six singular points on its yield surface which would lead to convergence difficulties in numerical calculations. The yield criterion of the modified Mohr–Coulomb model is described as follows:

$$F = \sigma_{\mathrm{m}} \sin\phi + \sqrt{\bar{\sigma} K^2(\theta) + m^2 c^2 \cos^2\phi} - c\cos\phi = 0, \quad (1)$$

where c and ϕ are, respectively, the cohesion and the internal angle of friction, σ_{m} is the average stress, $\bar{\sigma}$ is the equivalent stress, θ is the Lode angle, and m $(0 \le m \le 1)$ is the tensile strength parameter.

In order to eliminate the singularity, $K(\theta)$ is expressed as a piecewise function:

$$K(\theta) = \begin{cases} \mathrm{A} - \mathrm{B}\sin 3\theta, |\theta| > \theta_{\mathrm{T}}, \\ \cos\theta - \frac{1}{\sqrt{3}} \sin\phi \sin\theta, |\theta| \le \theta_{\mathrm{T}}, \end{cases} \quad (2)$$

where A, B and θ_{T} are constants.

Based on the influence of damage on the failure of materials described in fracture mechanics, a damage law is introduced to describe the formation of rock fragment. The stiffness of materials is assumed to reduce gradually to zero when the materials reach their ultimate strength. The stress-strain response of the material consists of three parts. Initially, the material response is linear elastic, which is followed by plastic yielding governed by the modified Mohr-Coulomb model. At the onset of damage, the load-carrying capacity is markedly reduced until rupture occurs. Once the damage occurs in the material, the characteristic of stress-strain behavior is governed by the evolution of the degradation of the stiffness. According to the Lemaitre's strain equivalent theory [21], the stress tensor in the material at any given time during an analysis is given by a scalar damage equation as:

$$\tilde{\sigma} = (1 - D)\sigma, \quad (3)$$

where D is a damage variable that denotes the damage level of material. It takes a value between 0 and 1, which corresponds, respectively, to an intact or undamaged state and a fully damaged state. In this paper, D is defined using a plastic damage model which assumes that damage evolution depends on the equivalent plastic strain [22, 23]. The definition of damage is given by

$$D = (\bar{\varepsilon}^{pl}/\bar{\varepsilon}_0^{pl} - 1)/\alpha, \quad (4)$$

where $\bar{\varepsilon}^{\mathrm{pl}}$ is the equivalent plastic strain, $\bar{\varepsilon}_0^{\mathrm{pl}}$ is the equivalent plastic strain at the onset of damage, α is the damage coefficient of the material which can be determined by $\bar{\varepsilon}_0^{\mathrm{pl}}$ and $\bar{\varepsilon}_{\mathrm{f}}^{\mathrm{pl}}$, the equivalent plastic strain at failure.

As revealed from the simulation results of rock-breaking process induced by TBM cutters [15], the rock under cutters and the rock between cutters have different mechanisms of fracture. Therefore, two different criteria are set to define the separation of the rock fragment. Due to the direct cutting action, damage firstly appears in the rock under cutters, followed by the damage propagation as indicated by Eq. (4). When $D = 1$, the rock loses its load-bearing capacity. Then, an isolated region is formed if all the surrounding material loses its load-bearing capacity. In an unconstrained state, the isolated rock will experience a large rigid-body displacement. Then, a separation criterion should be defined by setting the maximum allowable rigid-body displacement. Hence, the composite separation criteria can be described as follows:

$$D = 1 \quad \text{or} \quad U \ge U_{\max}, \quad (5)$$

where U is the displacement at the integration point and $U_{\max}$ is the maximum allowable rigid displacement which can be set according to the element size.

Fracture occurs when all of the nodes at any element meet the separation criteria. Once fracture occurs, the fractured elements are deleted from the mesh.

2.2 Cutterhead–Rock Interaction

During the tunneling process, cutters roll through the excavation face. Rock-breaking is induced by the interaction between cutterhead and rock. As the detailed modeling process of Cutterhead–Rock interaction has been elaborated in our previous article [24], only the key steps is to be introduced in brief description as follows.

The contact pair algorithm was employed to define the Cutterhead–Rock interaction. It enforces contact constraints using a penalty contact method, which searches for slave node penetrations in the current configuration, including node-into-face, node-into-analytical rigid surface, and edge-into-edge penetrations. The surface of each cutter and the node-based surface of the rock were set as an independent non-smooth contact pair. The former was defined as the master surface due to its high stiffness and the latter was defined as the slave surface. When the master surface moves across the deformable slave surface, the tangential behavior is described by the Coulomb friction model.

Due to the relatively high stiffness, the cutterhead was modeled as a rigid body with a reference point. Then, the motion of cutterhead can be controlled by applying advancing speed and rotary speed on the reference point. Additionally, simulating the cutterhead using the rigid body feature makes it possible to calculate the thrust and torque of cutterhead using the resulting reaction force and moment acting on the reference point [25].

3 Characteristics of Cutter Loads

For illustrating the method to determine cutterhead loads, the cutterhead used in the Water Supply Project in the middle of Jilin Province was taken as an example. The diameter of the cutterhead is 8 m. Fifty-six disc cutters, including thirty-six front cutters, eight center cutters and twelve gage cutters are installed at different radii on the cutterhead. Based on the models and methods introduced in Section 2, the dynamic process when the cutterhead excavated through the marble with a penetration of 11 mm was simulated, and the mechanical parameters of the rock is shown in Table 1. Based on the simulation results, the characteristics of loads were analyzed, and the determination method of loads were given.

Table 1 Material parameters of rock

Parameter	Value
Density (kg/mm^3)	2.5×10^{-6}
Young's modulus (MPa)	22500
Poisson's ratio	0.3
Friction angle (°)	46.5
Dilation angle (°)	46.5
UCS (MPa)	112

3.1 Random Cutter Forces

Firstly, based on the numerical model introduced in Section 2, the forces on each cutter are obtained from the simulation of the tunneling process. Then, the type and parameters of the distribution of cutter forces are analyzed by statistical method.

The forces acting on a disc cutter consist of three components, namely the normal force (F_N), the tangential force (F_R) and the side force (F_S). By statistical analyzing, it is found that the characteristics of forces acting on the cutters installed at different radii are similar. Here, we chose one cutter as the analysis object to study the characteristics of its cutting forces. Figure 1 shows the responses of the forces acting on the front cutter whose installation radius is 2.05 m.

As shown in Figure 1, affected by the quasi-brittleness of rock, the forces acting on the cutter present the step characteristic and show some randomness during the rock breaking process. This is consistent with the engineering practice. Cutter forces fluctuate strongly and can reach peaks that are a multiple of the average forces. Comparing Figure 1(a) and (b), it can be seen that the normal force and the tangential force change in a similar way. They fluctuate around the mean values of 173 kN and 12 kN, respectively. Correlation analysis reveals that the tangential force is highly correlated with the normal force, shown in Figure 2. As for the side force, it changes around zero with the force direction pointing inside or outside in random, see Figure 1(c). The ratio of statistical average value of these three forces is approximately$F_N : F_R : F_S = 21.9 : 1.6 : 1$. It indicates that the side and tangential force contributes little to breaking rock and the normal force is the predominant component of the cutter forces.

Furthermore, to know the distribution characteristics of cutter forces, Kolmogorov–Smirnov test was carried out on the force sequences. Figure 3(a) and (b) show that the normal and tangential forces on cutters approximately obey the lognormal distribution, with the standard deviation of 132 kN and 10 kN, respectively. It indicates that the cutter forces distribute in a high dispersion and the peak rock-breaking forces occur in a very low frequency.

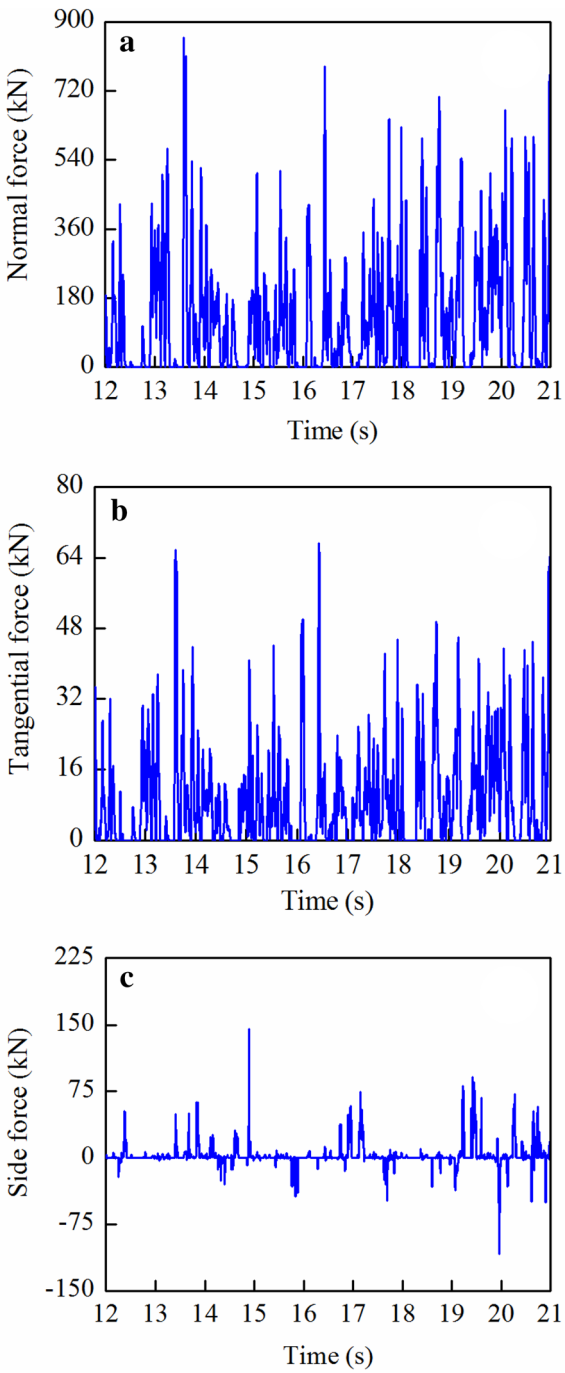

Figure 1 Curves of cutter forces with time changes: **a** normal force, **b** tangential force, **c** side force

Additionally, performing Kolmogorov–Smirnov test on the forces of both center cutters and gage cutters, results show that forces on all cutters approximately obey the

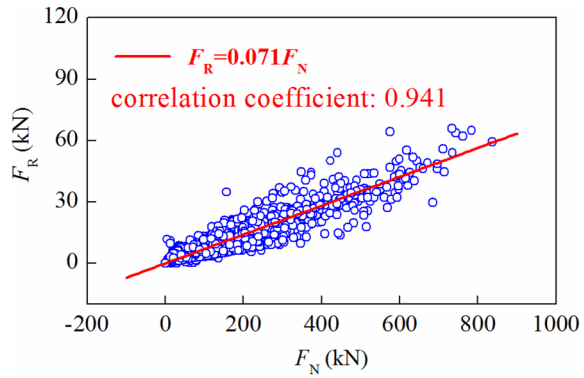

Figure 2 Correlation of tangential force and normal force

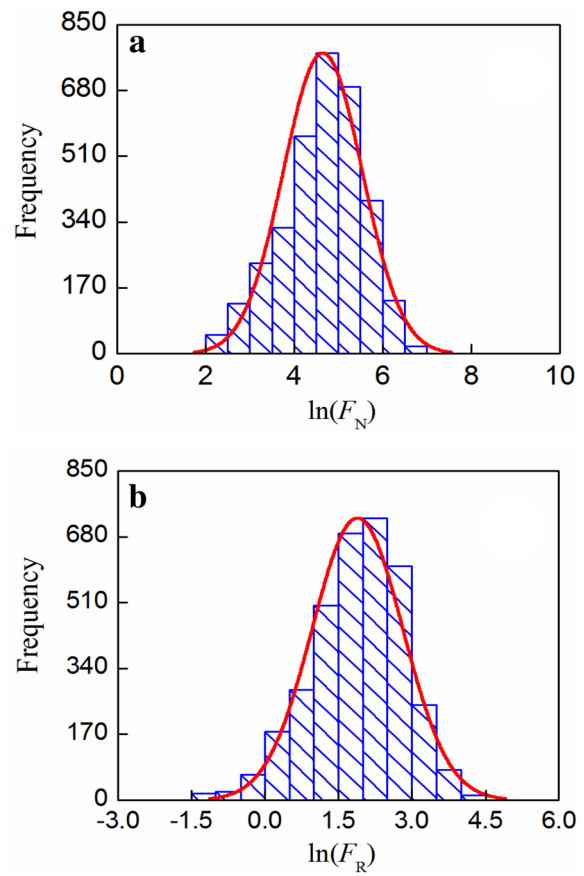

Figure 3 Histogram of the tangential and normal forces: **a** normal force, **b** tangential force

lognormal distribution. Meanwhile, the mean and standard deviation of each cutter's forces were obtained. Based on the distribution form, the mean and the standard deviation, the random forces on each cutter can be generated by using the Latin Hypercube Sampling method.

3.2 Characteristics of Cutterhead Loads

Based on the simulation model, the time-history curves for thrust and torque were generated, as shown in Figure 4. The loads on the whole cutterhead also fluctuate strongly during the excavation. In order to show the trend of loads clearly, a filter of a moving average of 255 points was used to smooth the simulation results. It is seen that the thrust and torque vary in a similar way. Both of them gradually increase at the beginning, then a relatively steady stage is achieved, in which the mean values of the thrust and torque are, respectively, 8909 kN and 1602 kN·m.

In addition, Kolmogorov–Smirnov test was carried out on the loads sequences to know their distribution characteristics. Figure 5(a) and (b) show that the thrust approximately obeys the normal distribution, while the torque approximately obeys the lognormal distribution.

3.3 A Three-Parameter Model for the Mean of Cutterhead Loads

In the stage of initial design, the cutterhead loads should be estimated according to the geological conditions and construction parameters. And upon the estimated loads, the main structural parameters of the cutterhead could be determined. To estimate cutterhead loads, it is

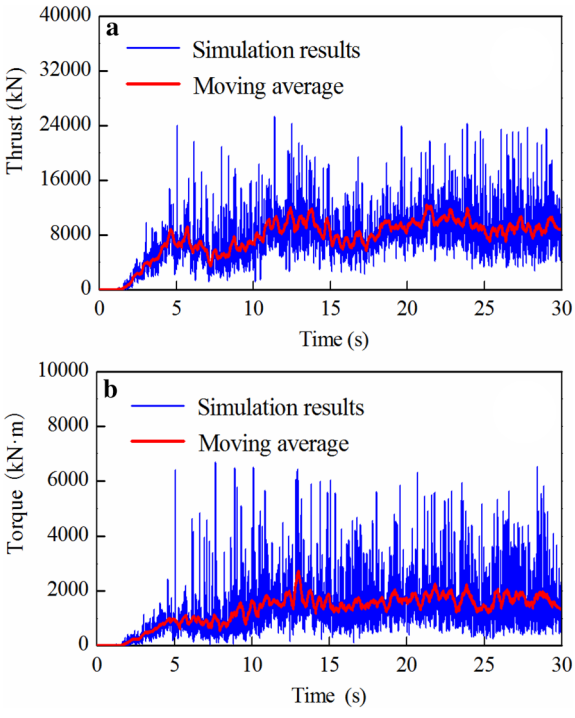

Figure 4 Curves of cutterhead loads with time changes: **a** thrust, **b** torque

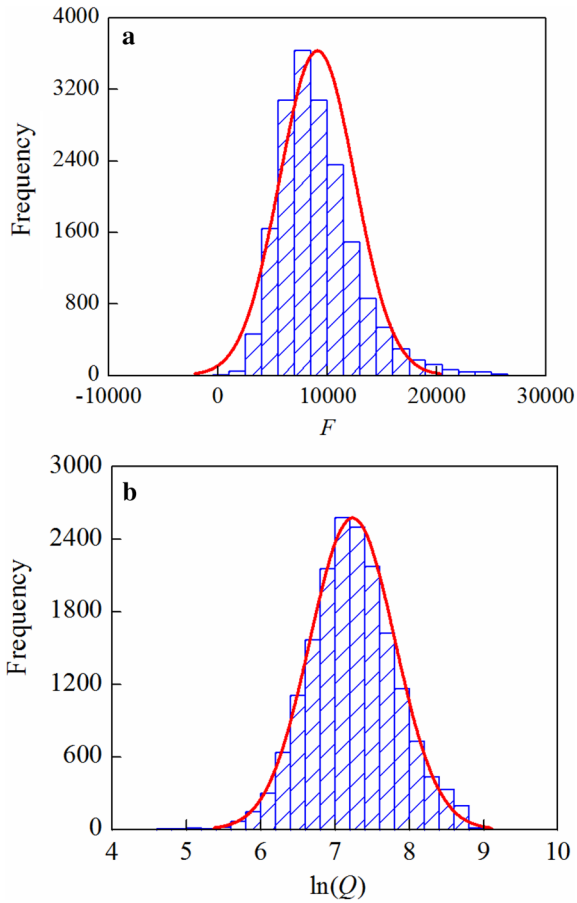

Figure 5 Histogram of cutterhead loads: **a** thrust represented by *F* (kN), **b** torque represented by *Q* (kN·m)

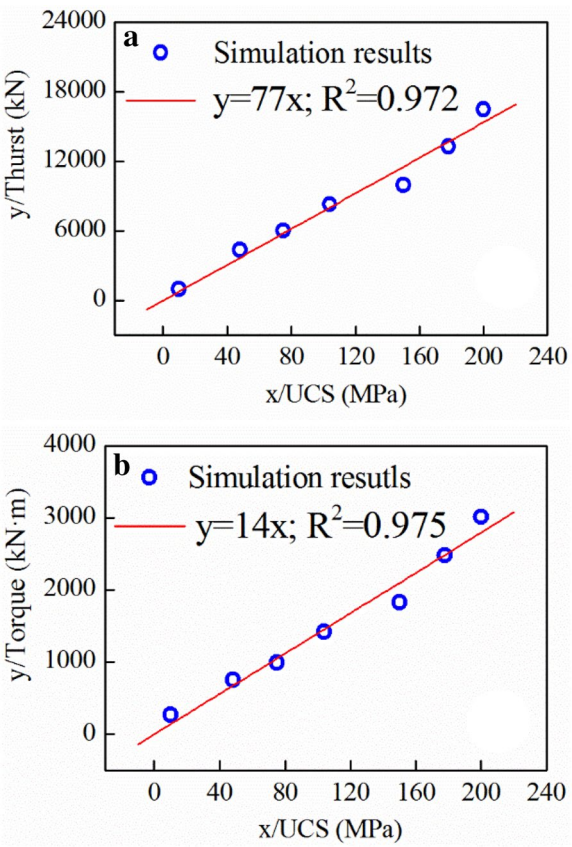

Figure 6 Relationships between the mean of cutterhead loads and UCS, **a** thrust, **b** torque

necessary to investigate the effects of different parameters on cutterhead loads.

Based on studying various geological parameters' effects on rock fragmentation, Gong et al. [26], concluded that the UCS is the most important factor. Moreover, the UCS directly determines the critical driving speed of the equipment [27]. Therefore, the UCS was selected as a variable to analyze the effect of geological parameters on cutterhead loads. A series of simulations were carried out for cutterhead tunneling in rocks with different UCS. By regression analysis on the mean of the simulated loads, the mean of both thrust and torque are proportional to the UCS of rock, as shown in Figure 6.

Penetration, which refers to the cutting depth when cutterhead rotates one circle, is a significant design parameter for TBM. The small penetration would reduce tunneling efficiency and the large one would affect the safety of construction by causing the severe vibration [26]. To investigate the effect of penetration on cutterhead loads, a series of simulations were carried out for cutterhead excavation with different penetrations. And the relationship between the penetration and the mean of cutterhead loads was derived by regression analysis. It reveals that the mean of cutterhead loads increase with the penetration in the form of a power function (as shown in Figure 7), and the exponent for the thrust is smaller than that for the torque.

The diameter of cutterhead is the fundamental parameter for TBM design. It directly determines the tunneling capacity and the application of the equipment. To analyze the effect of cutterhead's diameter on the cutterhead loads, the tunneling processes for cutterheads with different diameters were simulated. And to investigate the relationship between cutterhead's diameter and the mean of cutterhead loads, a regression analysis was performed using the least square method. Results reveal that the cutterhead loads increase with the diameter of cutterhead in the form of a power function, and the exponent for thrust is smaller than that for torque, see Figure 8.

Above analysis show that the mean of cutterhead loads are proportional to the UCS, also they change with the penetration and the diameter of cutterhead

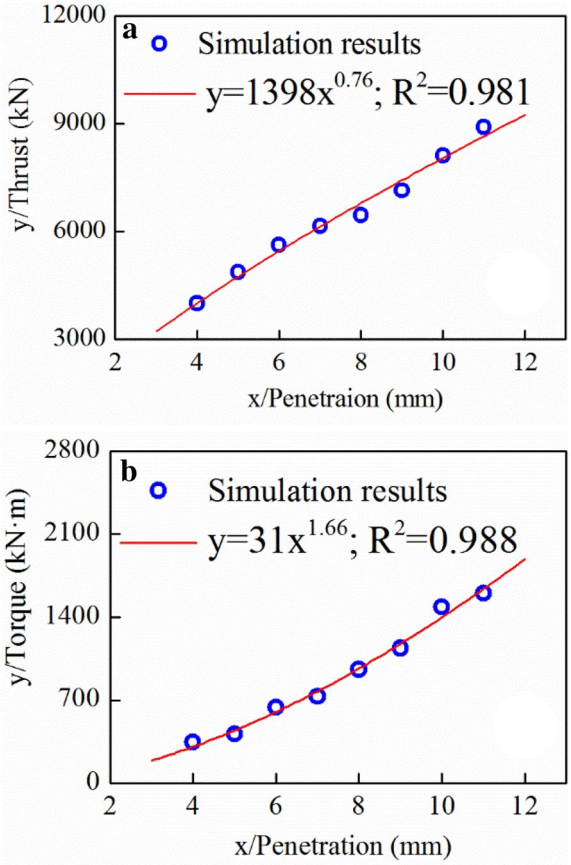

Figure 7 Relationships between the mean of cutterhead loads and penetration, **a** thrust, **b** torque

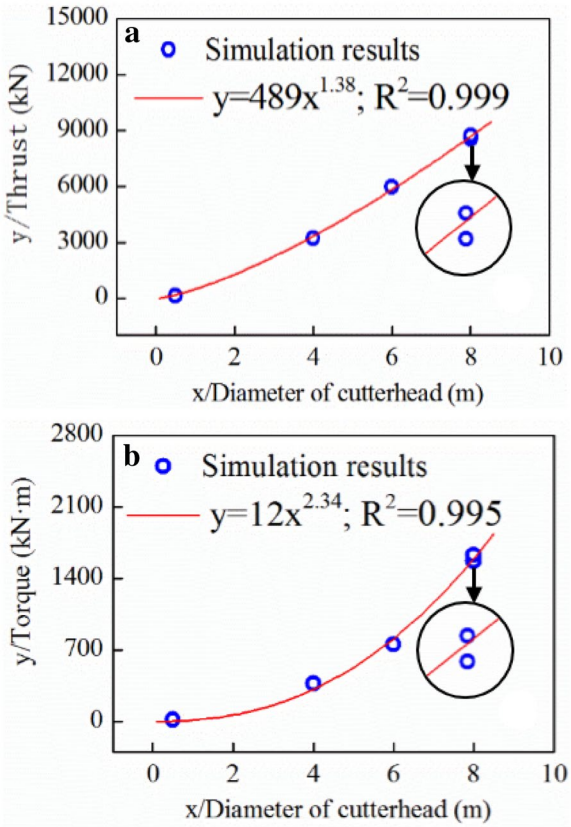

Figure 8 Relationships between the mean of cutterhead loads and cutterhead's diameter, **a** thrust, **b** torque

following a power function. Based on these results, the form of the model for the mean of cutterhead loads can be formulated as follows:

$$\begin{cases} F = a_1 C P^{b_1} D^{c_1}, \\ Q = a_2 C P^{b_2} D^{c_2}, \end{cases} \tag{6}$$

where F represents the thrust, Q represents the torque, C represents the UCS of rock, P represents the penetration, D represents the diameter of cutterhead, a_i, b_i, c_i $(i = 1, 2)$ are dimensionless constants to be determined.

By dimensional analysis, we have

$$c_1 = 2 - b_1,\ c_2 = 3 - b_2. \tag{7}$$

In order to determine the dimensionless constants, the cutterhead loads for 32 different sets of parameters were simulated; a regression analysis was performed on the mean of the loads using the least square method. Based on the regression results (see Figure 9), the dimensionless constants were determined, and the model for the mean of cutterhead loads was formulated as

$$\begin{cases} F = 0.147 C P^{0.73} D^{1.27},\ R^2 = 0.996, \\ Q = 0.262 C P^{1.39} D^{1.61},\ R^2 = 0.993, \end{cases} \tag{8}$$

where R^2 represents the goodness of fitting, $0 \le R^2 \le 1$.

This model provides the quantitative relationship between the mean of cutterhead loads and the core parameters of geology, operation and structure. Moreover, it is a reasonable non-dimensional model from the perspective of dimensional analysis.

Furthermore, data collected from one TBM tunneling project (the Water Supply Project in the middle of Jilin Province, China) was used to verify the effectiveness of the presented model. The engineering scenario is the construction of stake numbers from 21050 m to 21400 m. The major relevant geological strata identified in this area include sandstone, tuff, and granite, whose UCS ranges from 55 MPa to 130 MPa. The diameter of the cutterhead used in this project is 8 m. In addition, the operating parameters used in this analysis were automatically

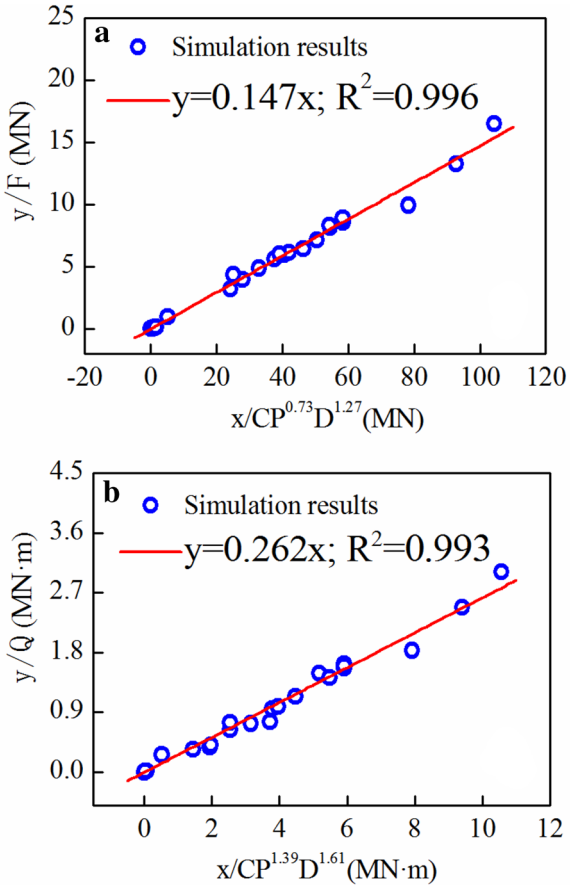

Figure 9 Regression analysis of the mean loads, **a** thrust, **b** torque

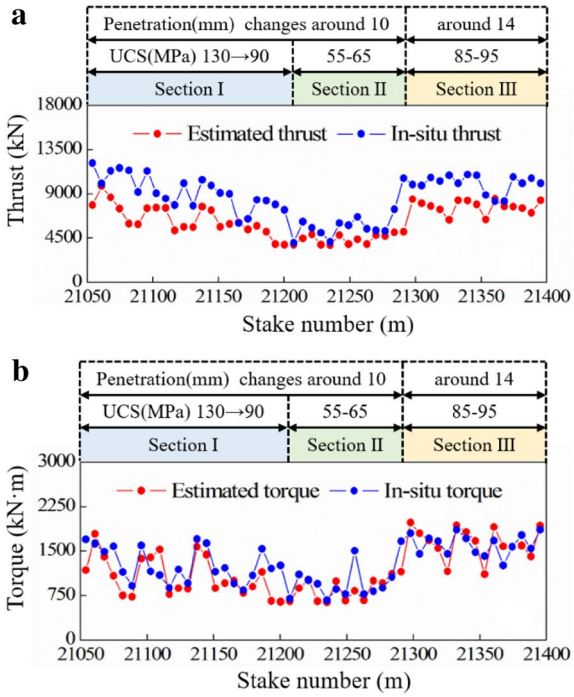

Figure 10 Comparison of the estimated results and the in-situ data: **a** thrust, **b** torque

recorded by the machine during tunneling, the penetration range is 6.2 mm to 16 mm.

Figure 10 shows a comparison of the estimated loads and the in-situ data (As the in-situ thrust and torque are both random in the tunnelling process, the mean value of data obtained in one ring is used for analysis). Since the proposed model considers the comprehensive effect of key parameters of geology, operation, and structure, the estimated loads follow the same trend of the in-situ loads.

As for the thrust, the estimated value is a little smaller than the in-situ data. The in-situ thrust refers to the equipment's total thrust, which includes the rock-breaking force acting on the cutterhead, the friction force of the shield, and the traction force of the subsequent equipment. While the estimated thrust only refers to the cutterhead's rock-breaking force, which is the major component of the total thrust. Therefore, the estimated thrust is smaller than the in-situ data. According to our calculation, the estimated cutterhead thrust accounts for 74.3% of the in-situ total thrust, which is consistent with engineering practice. As for the torque, the estimated value shows a good agreement with the measured data, and the mean of the relative error is 17.10%.

4 Case Applications

Based on the results of load research, the strength properties of a cutterhead used in the Water Supply Project in the middle of Jilin Province, was analyzed comprehensively. Firstly, in the stage of initial design, the static extreme loads evaluated by Eq. (8) were used for analyzing the structural strength preliminarily. Then, in the stage of detailed design, the failure probability of the cutterhead's strength was calculated under the random cutter forces, and the key factors of strength failure were analyzed. Finally, the dynamic loads obtained from tunneling simulation were employed to check the strength properties of the cutterhead with dynamical effects.

In the stage of the concept design, the main structural parameters of the cutterhead should be determined according to the results of strength analysis under the static extreme loads. Upon Eq. (8), the mean of cutterhead loads depends on the cutterhead's diameter (D), the UCS of rock (C) and the penetration (P). In this case, $D=8$ m, $C=112$ MPa, $P=0.011$ m. Substituting these parameters into Eq. (8), the mean of cutterhead loads can be calculated. To be safe, the scaling factor, which was set as 2, should be used to multiply the mean value. Then the extreme thrust and torque were determined as 17167

kN and 3163 kN·m, respectively. By applying the static extreme loads on the flange and fixing the front of each cutter ring, the strength analysis was performed on the cutterhead, and the result is shown in Figure 11.

Obviously, under the static extreme loads, the high stress appears in the stiffened panels of the cutterhead. The maximum equivalent stress is about 81 MPa, which is lower than the yield stress of Q345. It indicates that the design of the main structural parameters of the cutterhead meet the basic strength requirements.

Based on the analysis of the load characteristics, the rock-breaking forces on the cutters change in randomness, and approximately obey the lognormal distribution. Thus, in the stage of detailed design, it's necessary to calculate the failure probability of the cutterhead's strength under the random cutter forces. Meanwhile, the key factors of strength failure should be analyzed.

Upon the statistical characteristics of cutter forces, including the mean, the standard deviation and the correlation coefficient (listed in Table 2), a series of random forces were generated and set as the input variables. For evaluating the strength of cutterhead, the output variable was defined as

$$Z = \sigma_s - \sigma_{max}, \tag{9}$$

where σ_s represents the yield stress (as for Q345, $\sigma_s = 345$ MPa), σ_{max}represents the maximum equivalent stress. When $Z < 0$, strength failure occurs in the cutterhead.

Apply the generated random forces on each cutter and fix the flange. Then, by using the Monte Carlo method, the failure probability of the cutterhead's strength can calculated, and the result is shown in Figure 12. Obviously, $Z > 0$ occupies most of the distribution space, but there is also some space occupied by $Z < 0$. It indicated that strength failure occurred in the cutterhead under the random forces. By statistical analysis, the failure probability of the cutterhead's strength is 0.44%. In addition, the key factors resulting in the strength failure was analyzed by sensitivity analysis. It shows that the forces on the two front cutters with the maximum installed radii account two-thirds for the strength failure. In the stage of detailed design, the spacing of the outside front cutters should be optimized to improve the strength property of the cutterhead.

Finally, for checking the cutterhead's strength with dynamical effects and determining the failure position, a transient dynamic analysis was performed by applying the dynamic thrust and torque on the flange and fixing the front of each cutter ring. The dynamic cutterhead loads are obtained from the tunneling simulation, as shown in Figure 4 (the loads from 12 s to 21 s were selected for the analysis). Based the dynamic analysis, the stress responses of the dangerous node can be obtained, as presented in Figure 13.

It's shown that the stress on the dangerous node exceeds the yield stress of the material at 8 different time points, such as 12.88 s, 14.20 s and 19.80 s. Take 19.80 s as an example, the stress reaches the maximum value at this time, and the stress distribution on the local structure is shown in Figure 14. It can be found that the high stress is located on the middle of the stiffened panels, on which the stress failure would occurs during TBM excavation. Based on the simulation results, the structure was optimized, and the optimized cutterhead has been successfully applied to the construction.

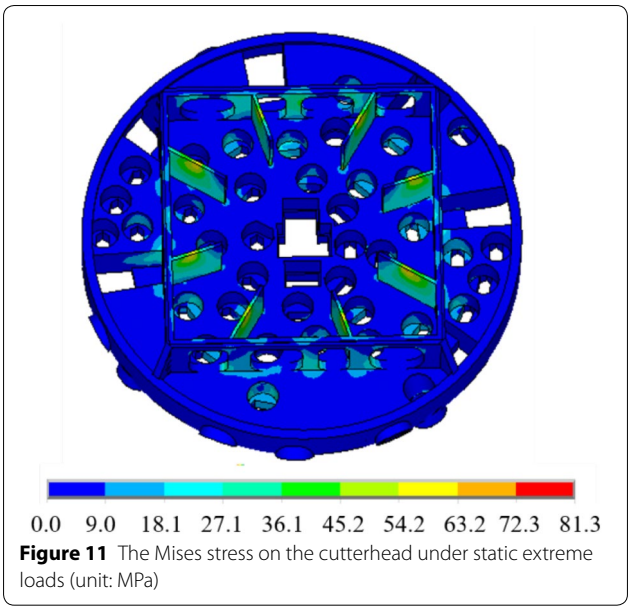

Figure 11 The Mises stress on the cutterhead under static extreme loads (unit: MPa)

5 Conclusions

To determine the cutterhead loads in TBM tunneling, a three-dimensional finite element model for Cutterhead–Rock interaction was developed. Based on the simulation results, the distribution characteristics of cutterhead loads and cutter forces were analyzed. Moreover, the effects of different parameters on cutterhead loads were discussed.

Results reveal that the cutter forces present the characteristics of a step change during the rock breaking process, and the responses of the forces show some randomness. The normal and tangential forces on cutters approximately have a lognormal distribution. And the tangential force is highly correlated with the normal force.

The cutterhead loads fluctuate strongly during the excavation, the thrusts are approximately distributed normally, while the torques approximately show the

Table 2 Distribution parameters of cutter forces

Installed radius (m)	F_R (kN)		F_N (kN)		Correlation coefficient	Installed radius (m)	F_R (kN)		F_N (kN)		Correlation coefficient
	Mean	Standard deviation	Mean	Standard deviation			Mean	Standard deviation	Mean	Standard deviation	
0.06	3.83	3.68	59.29	41.46	0.72	2.35	16.46	12.06	224.04	185.60	0.88
0.15	6.75	4.23	79.75	51.40	0.85	2.42	15.64	13.69	218.16	150.95	0.73
0.24	9.13	6.57	118.51	81.67	0.93	2.50	15.19	12.25	211.94	160.71	0.84
0.33	9.79	8.06	133.57	84.12	0.94	2.57	16.14	15.67	225.13	198.63	0.79
0.42	6.12	5.84	93.97	64.38	0.90	2.65	17.20	13.82	239.94	158.01	0.80
0.51	9.32	8.42	133.21	99.06	0.93	2.72	16.63	14.97	226.37	164.36	0.83
0.60	8.66	7.14	127.76	99.80	0.93	2.80	15.32	13.99	213.76	150.75	0.82
0.69	7.00	5.04	108.18	74.40	0.91	2.87	15.72	15.72	213.75	162.11	0.88
0.77	7.28	6.28	110.17	86.57	0.92	2.95	16.13	13.73	225.06	152.62	0.89
0.85	9.99	5.53	142.58	105.52	0.94	3.02	16.58	11.48	231.35	136.40	0.87
0.93	4.82	3.27	68.33	35.50	0.84	3.10	15.52	11.34	216.49	134.13	0.89
1.01	8.02	4.90	111.03	87.50	0.88	3.17	16.70	12.08	233.02	93.43	0.78
1.09	8.54	5.04	120.50	75.77	0.85	3.25	16.38	13.44	228.54	101.30	0.53
1.17	9.58	5.45	142.95	90.64	0.91	3.32	15.82	9.64	220.66	96.38	0.60
1.25	8.06	4.79	118.86	77.32	0.88	3.40	14.51	6.65	202.35	66.29	0.76
1.33	8.20	6.51	120.25	98.35	0.93	3.47	16.09	13.07	231.47	159.16	0.91
1.41	12.18	7.88	167.75	121.60	0.91	3.53	14.04	3.70	199.78	50.09	0.81
1.49	9.00	6.18	129.32	97.59	0.89	3.59	13.55	4.38	177.51	53.85	0.68
1.57	11.84	7.64	167.60	121.59	0.89	3.65	12.71	3.56	169.37	57.27	0.91
1.65	9.28	6.99	134.84	110.49	0.87	3.71	12.64	6.64	150.59	71.38	0.92
1.73	11.56	8.30	165.24	129.01	0.93	3.77	12.25	7.03	155.68	57.63	0.84
1.81	12.97	8.89	188.38	133.50	0.89	3.82	10.60	5.94	126.32	65.55	0.85
1.89	13.55	10.31	192.50	154.94	0.89	3.86	9.54	5.09	115.85	104.10	0.93
1.97	12.22	8.96	173.71	135.71	0.87	3.89	8.17	7.62	97.29	82.03	0.91
2.05	12.41	10.37	173.08	132.13	0.94	3.92	8.56	8.00	101.98	84.78	0.92
2.12	13.49	10.16	188.15	144.91	0.89	3.95	9.03	5.22	107.55	75.49	0.92
2.20	16.16	12.71	233.83	181.26	0.95	3.96	8.73	8.68	104.01	77.60	0.93
2.27	15.66	11.03	218.51	155.96	0.92	3.97	7.97	4.31	94.94	72.29	0.75

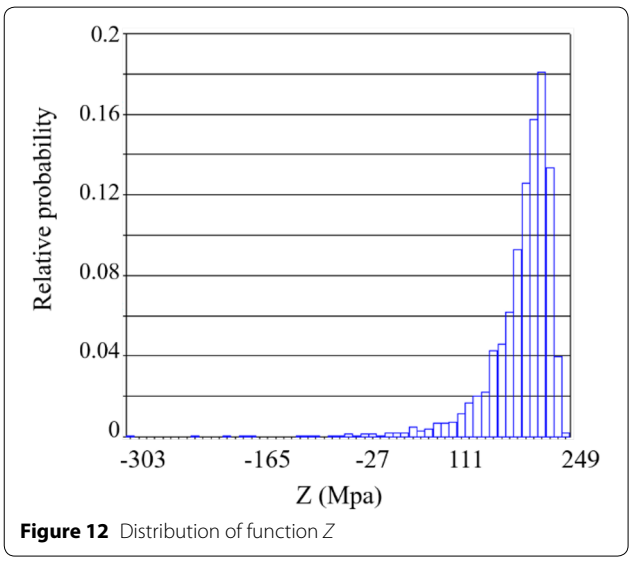

Figure 12 Distribution of function *Z*

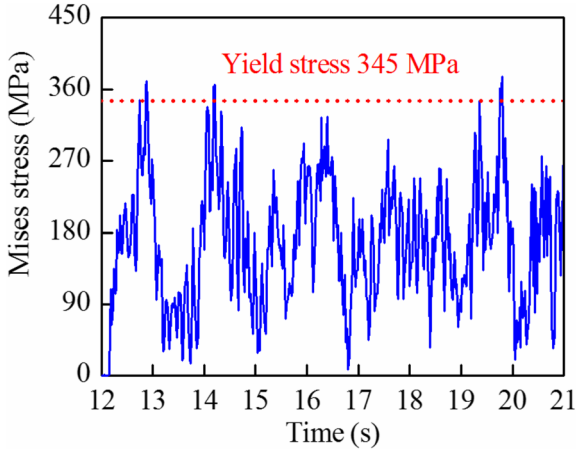

Figure 13 Response of stress on the dangerous node

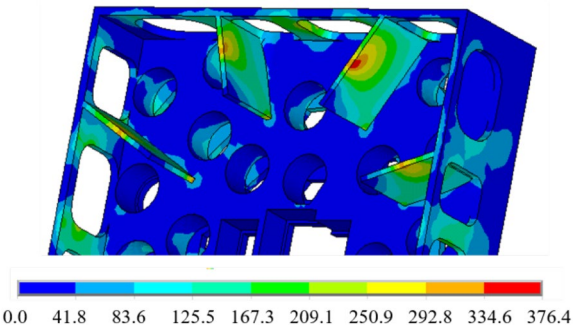

Figure 14 The distribution of Mises stress on the cutterhead when $t = 19.80$ s (unit: MPa)

lognormal distribution. In addition, the cutterhead loads are proportional to the UCS of rock, they also change with the penetration and the diameter of cutterhead following a power function. Based on these results, a dimensionless three-parameter model for the mean of cutterhead loads was proposed and its effectiveness is verified by comparing the estimated loads and the in-situ data.

A systematic method of strength analysis of the cutterhead was then developed based on the simulated loads. In the stage of initial design, the static extreme loads evaluated by Eq. (8) could be used to analyze the structural strength preliminarily. In the stage of detailed design, the random cutter forces generated by Monte Carlo method should be imposed to calculate the failure probability of the cutterhead's strength and to find the key factors of strength failure. Finally, the dynamic loads simulated under typical geology and operating parameters should be employed to check the strength properties with dynamical effects of the cutterhead.

Authors' Contributions

ZC conceived and designed the research methods and processes; MH was in charge of numerical simulation and data analysis; CQ assisted with writing the manuscript. All authors read and approved the final manuscript.

Authors' Information

Meidong Han, born in 1987, received his PhD from *Tianjin University, China* and is currently a lecturer at *Nanchang Hangkong University, China*. His research interest is numerical simulation in engineering.

Zongxi Cai, born in 1957, is currently a professor at *Tianjin University, China*. He received his PhD degree from *Tianjin University, China*, in 1992. His research interests include solid mechanics and structure engineering.

Chuanyong Qu, born in 1980, is currently an associate professor at *Tianjin University, China*. He received his PhD degree from *Tianjin University, China*, in 2007. His research interests include solid mechanics, fracture and fatigue and damage mechanics.

Funding

Supported by National Basic Research Program of China (973 Program, Grant No. 2013CB035042) and the National Natural Science Foundation of China (Grant No. 11672202).

Competing Interests

The authors declare that they have no competing interests.

Author Details

[1] School of Aircraft Engineering, Nanchang Hangkong University, Nanchang 330063, China. [2] School of Mechanical Engineering, Tianjin University, Tianjin 300350, China.

Received: 20 January 2019 Accepted: 15 November 2019
Published online: 04 December 2019

References

[1] J Wei, Q Sun, W Sun, et al. Load-sharing characteristic of multiple pinions driving in tunneling boring machine. *Chinese Journal of Mechanical Engineering*, 2015, 28(4): 801-809.
[2] J Z Huo, D Zhu, G Q Li, et al. Application of a small-timescale fatigue, crack-growth model to the plane stress/strain transition in predicting the lifetime of a tunnel-boring-machine cutter head. *Engineering Failure Analysis*, 2017, 71: 11-30.
[3] F F Roxborough, H R Phillips. Rock excavation by disc cutter. *International Journal of Rock Mechanics and Mining Sciences & Geomechanics Abstracts*, 1975, 12(12): 361-366.
[4] J Rostami, L Ozdemir. A new model for performance prediction of hard rock TBMs. *Proceedings of the Rapid Excavation and Tunneling Conference*, Boston, America, June 13-17, 1993: 793-793.
[5] G Li, L D Zhu, J Y Yang, et al. A method to predict disc cutter wear extent for hard rock TBMs based on CSM model. *China Mechanical Engineering*, 2014, 25(1): 32-35. (in Chinese)
[6] J Q Liu, J B Ren, W Guo. Thrust and torque characteristics based on a new cutter-head load model. *Chinese Journal of Mechanical Engineering*, 2015, 28(4): 801-809.
[7] J Z Huo, N Hou, W Sun, et al. Analyses of dynamic characteristics and structure optimization of tunnel boring machine cutter system with multi-joint surface. *Nonlinear Dynamics*, 2017, 87(1): 237-254.
[8] Y M Xia, T Ouyang, X M Zhang, et al. Mechanical model of breaking rock and force characteristic of disc cutter. *Journal of Central South University*, 2012, 19(7): 1849-1852.
[9] J Z Huo, W Z Wang, W Sun, et al. The multi-stage rock fragmentation load prediction model of tunnel boring machine cutter group based on dense core theory. *The International Journal of Advanced Manufacturing Technology*, 2017, 90(1-4): 277-289.
[10] Q Geng, Z Y Wei, H Meng. An experimental research on the rock cutting process of the gage cutters for rock tunnel boring machine (TBM). *Tunnelling and Underground Space Technology*, 2016, 52: 182-191.
[11] Q Geng, Z Y Wei, H Meng, et al. Free-face-assisted rock breaking method based on the multi-stage tunnel boring machine (TBM) cutterhead. *Rock Mechanics and Rock Engineering*, 2016, 49(11): 4459-4472.
[12] Y M Xia, Y C Tian, Q Tian, et al. Side force formation mechanism and change law of TBM center cutter. *Journal of Central South University*, 2016, 23: 1115-1122.
[13] Q Tan, K Zhang, Y M Xia, et al. Three-dimensional simulation of rock breaking by TBM cutter. *Journal of Shandong University (Engineering Science)*, 2009, 39(06): 72-77. (in Chinese)
[14] Q M Gong, Y Y Jiao, J Zhao. Numerical modeling of the effects of joint spacing on rock fragmentation by TBM cutters. *Tunneling and Underground Space Technology*, 2006, 21(1): 46-55.
[15] Q M Gong, J Zhao, A M Hefny. Numerical simulation of rock fragmentation process induced by two TBM cutters and cutter spacing optimization. *Tunnelling and Underground Spacing Technology*, 2006, 21(3/4): 263-270.
[16] S Y Zhou, Y L Kang, C X Su, et al. Mechanical analysis and prediction for the total thrust on TBMs. *International Conference on Intelligent Robotics and Applications*, Portsmouth, UK, August 24-27, 2015: 436-444.

[17] I Farmer, P Garrity, N H Glossop. Operational characteristics of full face tunnel boring machines. *Proceedings of the Rapid Excavation and Tunneling Conference*, New Orleans, America, June 14-17, 1987: 188-201.
[18] P P Nelson, Y A Jalil, C Laughton. Analysis of performance measures of tunnel boring machines. *Proceedings of the ISRM Symposium*, Chester, UK, September 14-17, 1992: 408-413.
[19] U Ates, N Bilgin, H Copur. Estimating torque, thrust and other design parameters of different type TBMs with some criticism to TBMs used in Turkish tunnelling projects. *Tunnelling and Underground Space Technology*, 2015, 40: 46-63.
[20] S P Jia, W Z Chen, J P Yang. An elastoplastic constitutive model based on modified Mohr-Coulomb criterion and its numerical implementation. *Rock and Soil Mechanics*, 2010, 31(7): 2051-2058. (in Chinese)
[21] J Lemaitre. How to use damage mechanics. *Nuclear Engineering and Design*, 1984, 80(2): 233-245.
[22] J Lubliner, J Oliver, S Oiler, et al. A plastic-damage model for concrete. *International Journal of Solids and Structures*, 1989, 25(3): 299-326.
[23] J Lee, G L Fenves. A plastic-damage concrete model for earthquake analysis of dams. *Earthquake Engineering & Structural Dynamics*, 1998, 27(9): 937-956.
[24] M D Han, Z X Cai, C Y Qu, et al. Dynamic numerical simulation of cutterhead loads in TBM tunnelling. *Tunnelling and Underground Space Technology*, 2017, 70: 286-298.
[25] M Abo-Elnor, R Hamilton, J T Boyle. 3D dynamic analysis of soil-tool interaction using the finite element method. *Journal of Terramechanics*, 2003, 40(1): 51-62.
[26] Q M Gong, J Zhao. Development of a rock mass characteristics model for TBM penetration rate prediction. *International Journal of Rock Mechanics and Mining Sciences*, 2009, 46(1): 8-18.
[27] M D Han, Z X Cai, C Y Qu. Study on the critical driving speed of the tunnel boring machine cutterhead based on the dynamic stability. *Journal of Mechanical Engineering*, 2014, 50(21): 10-16. (in Chinese)